OXFORD

Human Molecular Genetics, 2015, Vol. 24, No. 17 4948–4957

doi: 10.1093/hmg/ddv216
Advance Access Publication Date: 9 June 2015
Original Article

ORIGINAL ARTICLE

Reversibility of neuropathology and motor deficits in an inducible mouse model for FXTAS

Renate K. Hukema[1,*,†], Ronald A.M. Buijsen[1,†], Martijn Schonewille[2,†], Chris Raske[4], Lies-Anne W.F.M. Severijnen[1], Ingeborg Nieuwenhuizen-Bakker[1], Rob F.M. Verhagen[1], Lisanne van Dessel[1], Alex Maas[3], Nicolas Charlet-Berguerand[6], Chris I. De Zeeuw[2,7], Paul J. Hagerman[4], Robert F. Berman[5,‡] and Rob Willemsen[1,‡]

[1]Department of Clinical Genetics, [2]Department of Neuroscience and [3]Department of Cell Biology, Erasmus MC, 3000 CA Rotterdam, The Netherlands, [4]Department of Biochemistry and Molecular Medicine and [5]Department of Neurological Surgery, School of Medicine, University of California Davis, CA 95618, USA, [6]IGBMC, 67404 Illkirch, France and [7]The Netherlands Institute for Neuroscience, Amsterdam 1105 BA, The Netherlands

*To whom correspondence should be addressed at: Department of Clinical Genetics, Erasmus MC, Room Ee971, PO Box 2040, 3000 CA Rotterdam, The Netherlands. Tel: +31 107030684; Email: r.hukema@erasmusmc.nl

Abstract

Fragile X-associated tremor/ataxia syndrome (FXTAS) is a late-onset neurodegenerative disorder affecting carriers of the fragile X-premutation, who have an expanded CGG repeat in the 5′-UTR of the *FMR1* gene. FXTAS is characterized by progressive development of intention tremor, ataxia, parkinsonism and neuropsychological problems. The disease is thought to be caused by a toxic RNA gain-of-function mechanism, and the major hallmark of the disease is ubiquitin-positive intranuclear inclusions in neurons and astrocytes. We have developed a new transgenic mouse model in which we can induce expression of an expanded repeat in the brain upon doxycycline (dox) exposure (i.e. Tet-On mice). This Tet-On model makes use of the PrP-rtTA driver and allows us to study disease progression and possibilities of reversibility. In these mice, 8 weeks of dox exposure was sufficient to induce the formation of ubiquitin-positive intranuclear inclusions, which also stain positive for the RAN translation product FMRpolyG. Formation of these inclusions is reversible after stopping expression of the expanded CGG RNA at an early developmental stage. Furthermore, we observed a deficit in the compensatory eye movements of mice with inclusions, a functional phenotype that could be reduced by stopping expression of the expanded CGG RNA early in the disease development. Taken together, this study shows, for the first time, the potential of disease reversibility and suggests that early intervention might be beneficial for FXTAS patients.

Introduction

Fragile X-associated tremor/ataxia syndrome (FXTAS) is a late-onset neurodegenerative disorder causing tremor, ataxia, brain atrophy, cognitive loss, dementia and, in some individuals, early death. This disorder develops in individuals, referred to as fragile X-premutation carriers, who have an expansion of 55–200 CGG repeats in the 5′-UTR of the *FMR1* gene (1). The prevalence of premutation carriers in the general population is high and is

†The authors wish to be known that, in their opinion, the first three authors should be regarded as joint First Authors.
‡The authors wish to be known that, in their opinion, the last two authors should be regarded as joint Last Authors.
Received: May 1, 2015. **Revised and Accepted:** June 4, 2015

estimated 1:291 for females and 1:855 for males (2). The chances of developing FXTAS increase dramatically with age, with approximately 45.5% of male and 16.5% of female premutation carriers over the age of 50 developing FXTAS (3). The major hallmark of FXTAS neuropathology is the presence of intranuclear inclusions that stain for ubiquitin in neurons and astrocytes throughout the brain (4). Premutation carriers with or without FXTAS show elevated levels of *FMR1* mRNA and normal-to-slightly reduced levels of FMRP protein (5). This finding has led to the proposal that FXTAS is caused by a toxic RNA gain-of-function mechanism, in which mutant RNA containing the expanded CGG repeat would be pathogenic (6). An additional mechanism of toxicity that is triggered by (expanded) CGG repeats involves repeat-associated non-AUG (RAN) translation of the CGG repeat and has been proposed to play a role in FXTAS (7). Mutant RNA bearing a CGG repeat expansion can be translated into protein without using a traditional AUG start codon, and such translation may occur in all three reading frames (i.e. CGG, GGC or GCG) leading to multiple toxic entities from a single repeat expansion. For the CGG repeat in FXTAS, it has been proposed (8) that RAN translation initiates in the 5′-UTR of the *FMR1* gene and results in the production of a polyglycine (FMRpolyG) and also a polyalanine (FMRpolyA) protein. The presence of FMRpolyG was demonstrated in cell culture, *Drosophila* and mouse models and brain and other tissues from FXTAS patients, whereas FMRpolyA could only be detected in transfected cells (8,9).

Previously, we and others have generated knock-in mouse models with expanded CGG repeats that have greatly facilitated the study of FXTAS disease progression (10,11). In our knock-in mouse model, the murine 8CGG repeat has been replaced by homologous recombination in ES cells with a human expanded 98CGG (12). This model recapitulates many of the features seen in human FXTAS: not only increased expression of *Fmr1* mRNA, decreased levels of FMRP and intranuclear aggregates in neurons and astrocytes, but also poor motor function, impaired memory and progressive spatial processing deficits (13). Recently, we reported initial findings in our new Tet-On doxycycline-inducible mouse model for FXTAS (14). In this model, expression of either a control size CGG repeat (11CGGs) or a pathogenic expanded repeat (90CGGs) can be activated using the Tet-On system. In this initial study, we reported toxic effects of expression of the expanded repeat under control of the ubiquitous hnRNP-rtTA driver. We showed that RNA containing an expanded CGG repeat is pathogenic in the liver, whereas RNA containing a control-sized repeat is not. After 5 days of doxycycline (dox) exposure, the expression of expanded repeat RNA resulted in mitochondrial dysfunction in the liver and early death, hampering the possibility to study the long-term effects of expanded CGG repeat expression in brain. Importantly, the observed effects were due to the ectopically expressed expanded repeat, out of the context of the *Fmr1* gene.

Results

Inducible expression of expanded CGG RNA in the brain

Recently, we have shown that induced expression of an expanded 90CGG RNA produces mitochondrial stress and apoptosis in the liver in a Tet-On mouse model for FXTAS (14). Here, we used the same strategy to create bigenic transgenic mice in which exposure to dox induces expression of either a control size 11CGG or an expanded 90CGG repeat RNA fused to an enhanced green fluorescent protein (eGFP) reporter in the brain. These mice were created by crossing our new PrP-rtTA 'driver' mouse line with 'target' mouse lines carrying a tetracycline response element (TRE) linked to either an 11CGG (TRE-11CGG-eGFP) or 90CGG (TRE-90CGG-eGFP) repeat expansion and an eGFP reporter (Fig. 1A). We opted for the prion protein or PrP promoter, as it drives expression confined to the central nervous system (both neurons and glia cells). We expected that the use of this driver line would avert the liver failure we observed when using the more ubiquitous driver line hnRNP-rtTA (14). Indeed, the double transgenic TRE-nCGG-eGFP/PrP-rtTA mice could be treated with dox in their drinking water for as long as 28 weeks without signs of overt toxicity. Dox treatment resulted in eGFP expression throughout the brain as expected, but with the strongest expression in the cerebellum, hippocampus and striatum (Fig. 2). We could detect eGFP expression in the brain within 2 days after the start of dox treatment. Thus dox can quickly and efficiently cross the blood–brain barrier to activate transgene expression in brain tissue. Lack of eGFP expression in single transgenic TRE-nCGG-eGFP mice treated with dox and double transgenic TRE-nCGG-eGFP/PrP-rtTA mice without dox provides clear evidence that the Tet-On system did not show leaky expression (Supplementary Material, Fig. S1). We also found that 90CGG RNA levels were slightly lower than 11CGG RNA levels (Fig. 1B), which could be explained by different integration sites of the transgenes, as an untargeted approach used to generate the mouse lines 90CGG RNA in brain homogenates was about two times overexpressed when compared with endogenous *Fmr1* levels (Supplementary Material, Fig. S2). Because these RNA levels were in whole brain homogenates and the expression pattern is a mosaic of expressing and non-expressing cells present, the effect of overexpression per expressing cell would be much more dramatic.

Expanded CGG RNA expression leads to inclusion formation

The major hallmark of FXTAS is the presence of ubiquitin-positive intranuclear inclusions throughout the brain. Thus, after inducing transgene expression in the brains of bigenic mice by dox exposure through drinking water (4 mg/ml), we studied the distribution and morphology of ubiquitin-positive inclusions. Initially, we started our histological analysis after 8 weeks

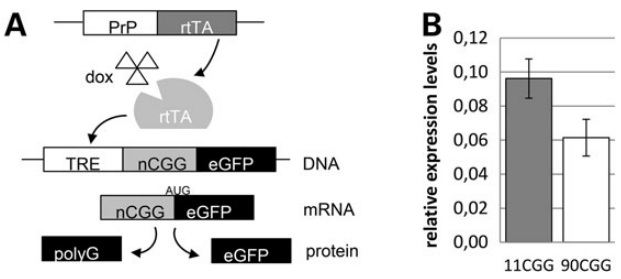

Figure 1. Dox-induced expression of nCGG-eGFP in the brain. (**A**) The Tet-On system was used to generate bigenic mice expressing an 11CGG or 90CGG repeat at the RNA level. Expression of rtTA is controlled by the PrP promoter on a separate transgene. Upon dox administration, rtTA will be activated and can bind the Tet response element on another transgene, which induces expression of the nCGG repeat at the RNA level and eGFP at the protein level. As the transgene contains the 5′-UTR of the *FMR1* gene, a polypeptide is formed from the repeat by RAN translation. (**B**) Quantitative RT-PCR on RNA isolated from the brain of dox-treated (16–28 weeks) bigenic TRE-nCGG-eGFP/PrP-rtTA mice. 90CGG RNA levels are lower than 11CGG RNA levels in whole brain homogenates ($N = 8$). Error bars represent SEM.

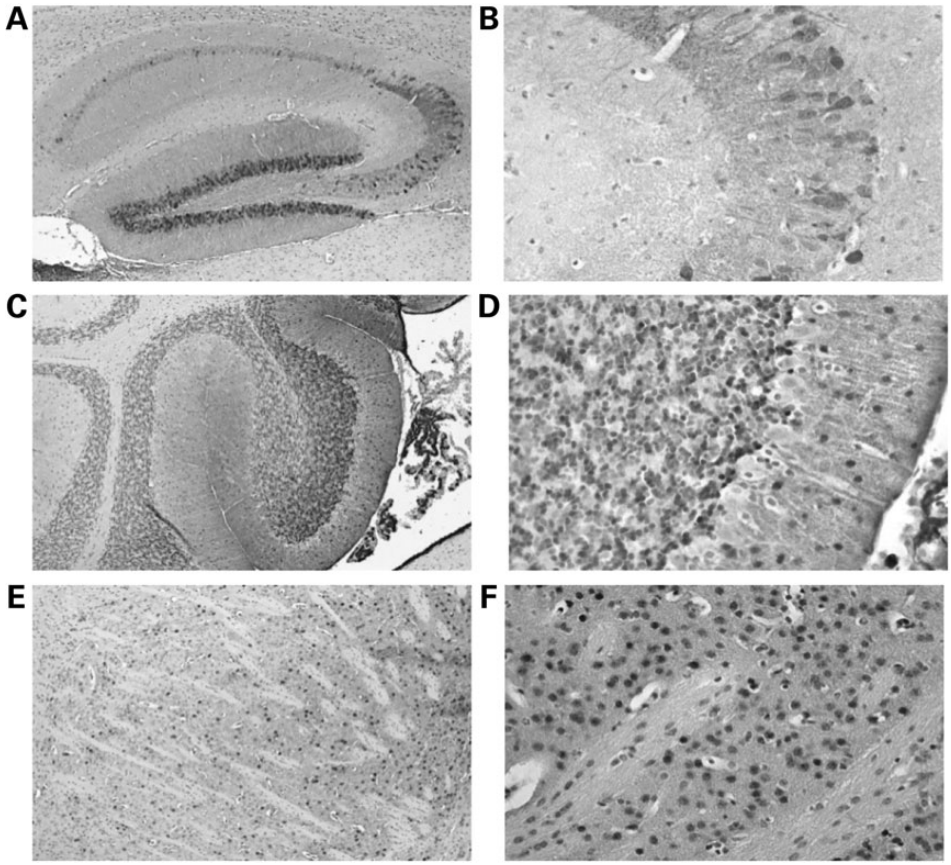

Figure 2. eGFP expression in brain after dox induction of bigenic TRE-nCGG-eGFP/PrP-rtTA mice. Immunohistochemical staining of paraffin section of brain from dox-induced nCGG-eGFP-expressing mice in (**A**) hippocampus (10×), (**B**) mainly in the CA3 area (40×); (**C**) cerebellum (40×), (**D**) mainly in lobule X (100×) and (**E**) striatum 10× and (**F**) striatum 40×.

of dox treatment. In all areas of the brains of TRE-90CGG-eGFP/PrP-rtTA mice that showed eGFP expression, and thus the expanded 90CGG RNA, we detected ubiquitin-positive intranuclear inclusions (Fig. 3). As expected, most intranuclear inclusions were found in those brain regions expressing high levels of eGFP, including lobule X of the cerebellum, hippocampus and striatum. In hippocampus, round/spherical inclusions were found, with the largest in the CA3 area (Fig. 3A). In contrast, in the granular layer of lobule X of the cerebellum, inclusions showed a cat-eye shape (Fig. 3E–H). Despite differences in shape, the inclusions were always intranuclear and only one per nucleus was observed. Ubiquitin-positive inclusions were never observed in mice expressing 11CGG RNA, not even after as long as 28 weeks of dox induction, nor in bigenic mice not treated with dox (Supplementary Material, Fig. S3A). The level of RNA expression was lower for 90CGG than for 11CGG, suggesting that the formation of inclusions is dependent on the presence of expanded CGG RNA and is not caused by overexpression of CGG RNA *per se*.

The formation of inclusions was followed over time by treating the bigenic TRE-90CGG-eGFP/PrP-rtTA mice for different time periods with dox. The percentage of neurons with an inclusion was quantified by analysis of 500 nuclei in the granular cell layer of cerebellar lobule X. In this area of the brain, the expression of eGFP was most pronounced and showed the least variation. Also, the first ubiquitin-positive inclusions were observed in this part of the brain after 6 weeks of dox exposure. After 8 weeks of dox treatment, 27% (with an SEM of 7%) of the nuclei showed an ubiquitin-positive inclusion, with a significant increase over time to 70% (with an SEM of 3%) after 28 weeks of dox treatment (Fig. 4A). In addition, not only the number of inclusions increased, but also the size increased with longer dox exposure times. Specifically, the size increased from 0.79 µm (with an SEM of 0.07) at 8 weeks treatment to 1.91 µm (with an SEM of 0.21) at 28 weeks of dox induction (Fig. 4B). Thus, prolonged expression of expanded CGG RNA results in higher number of and larger-sized inclusions.

Polyglycine and other components of the inclusions

Recently, a new type of translation has been described for several repeat-associated diseases, including FXTAS (8). This repeat-associated non-AUG (RAN) translation is thought to be induced by the presence of an expanded repeat in some RNAs. The repeat expansion is thought to stall scanning of the mRNA by the 40S ribosomal subunit, resulting in the use of an alternate downstream non-AUG start site. This, in turn, could cause a frameshift and translation of polypeptides associated with the CGG repeat expansion. As a result, different polypeptides could theoretically be produced from RAN translation of the CGG repeat (polyArg, polyGly and polyAla), depending on the reading frame (i.e. CGG, GGC or GGC). For FXTAS, such translation has been reported to result in the production of poly-glycine (FMRpolyG) and poly-alanine (FMRpolyA) peptides (8). We have used two different antibodies to detect FMRpolyG: 8FM and 9FM. The 8FM is specific

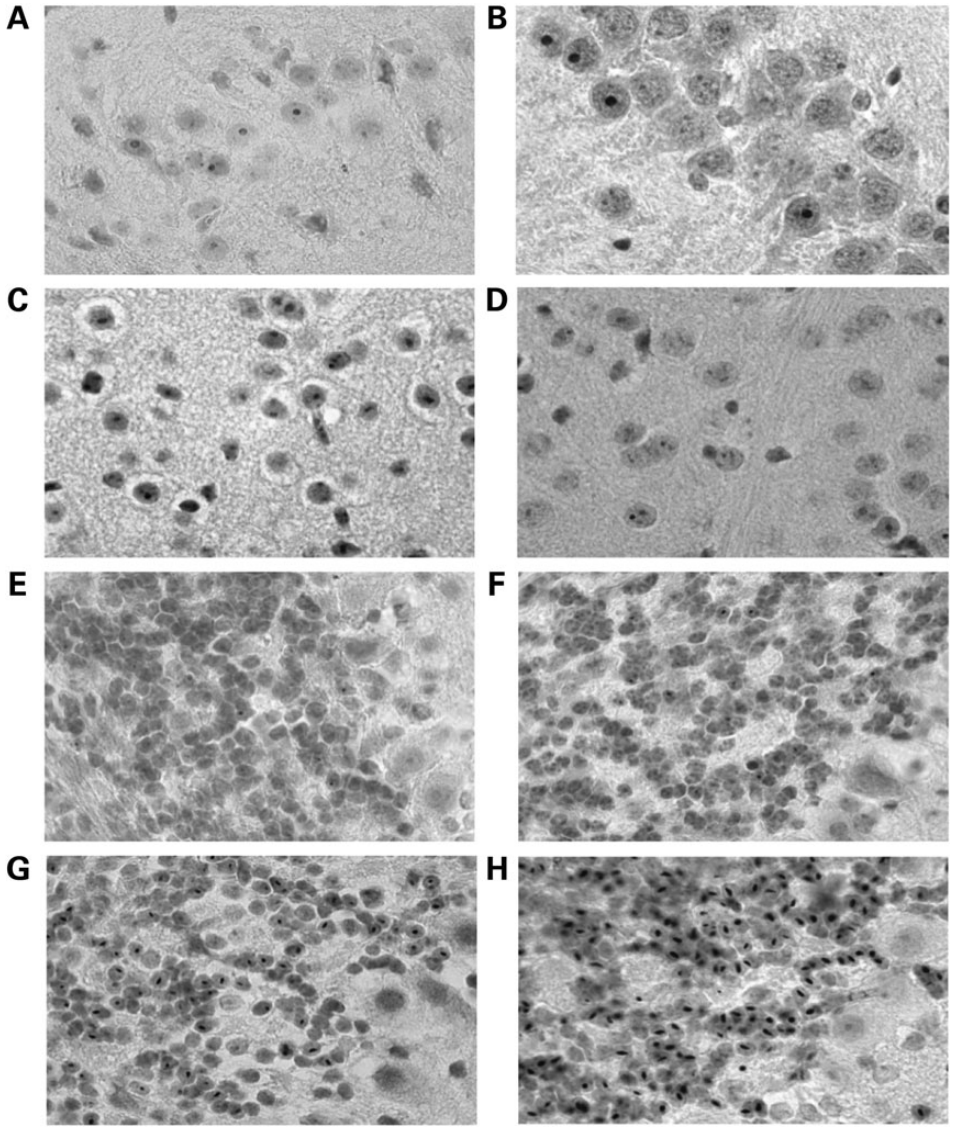

Figure 3. Ubiquitin and FMRpolyG-positive intranuclear inclusions in different brain areas after dox induction of bigenic TRE-90CGG-egFP/PrP-rtTA mice. (**A**) Ubiquitin-positive intranuclear inclusions in CA3 of the hippocampus. (**B**) FMRpolyG-positive intranuclear inclusions in CA3 of the hippocampus. (**C**) Ubiquitin-positive intranuclear inclusions in striatum. (**D**) FMRpolyG-positive intranuclear inclusions in striatum. (**E**) Ubiquitin-positive intranuclear inclusions in the granular cell layer of lobule X after 8 weeks of dox induction. (**F**) FMRpolyG-positive intranuclear inclusions in the granular cell layer of lobule X after 8 weeks of dox induction. (**G**) Ubiquitin-positive intranuclear inclusions in the granular cell layer of lobule X after 20 weeks of dox induction. (**H**) FMRpolyG-positive intranuclear inclusions in the granular cell layer of lobule X after 20 weeks of dox induction. All images, 100× magnification.

for the sequence directly upstream of the polyG tract, and 9FM is specific for the sequence directly downstream of the polyG tract (9). Thus both antibodies are specific for polyG translated from the GGC tract in *Fmr1* mRNA. Both the 90CGG and 11CGG repeat transgenes in our dox-inducible mice are of human origin, and they also contain some human flanking sequences that include the sequence used as the epitope for these antibodies. Therefore, we explored the presence of FMRpolyG in the brain of the inducible mice. FMRpolyG-positive inclusions were present in those brain regions of 90CGG mice that express high levels of eGFP, whereas 11CGG mice were totally devoid of FMRpolyG-positive inclusions (Fig. 3 and Supplementary Material, Fig. S3B). The FMRpolyG-positive inclusions could be detected with both 8FM and 9FM antibodies. As both antibodies achieved similar results, we continued our studies using the 8FM antibody only (Supplementary Material, Fig. S4). All brains that were studied for the presence of ubiquitin-positive inclusions were also analyzed for the presence of FMRpolyG. The distribution of the FMRpolyG inclusions was similar to the ubiquitin inclusions. Co-localization studies of ubiquitin and FMRpolyG using double immunofluorescence staining demonstrated a complete co-localization in all inclusions at all time points examined (Fig. 5). We never observed inclusions that stained positive only for ubiquitin or only for FMRpolyG.

In addition, to further characterize the nature of the intranuclear inclusions, we studied the localization of proteins previously shown to be components of these inclusions (12,15). We confirmed the presence of the 20S core complex of the proteasome, Hsp40 and Rad23B (Fig. 5). Similar to FMRpolyG, these components almost always show co-localization with ubiquitin.

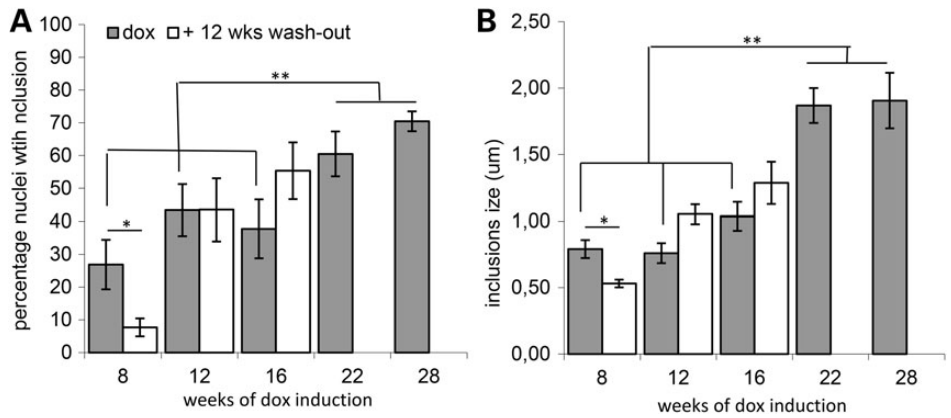

Figure 4. Quantification of ubiquitin-positive intranuclear inclusions in cerebellar lobule X of TRE-90CGG-eGFP/PrP-rtTA mice. (**A**) The percentage of nuclei containing ubiquitin-positive inclusions after different dox treatment periods. (**B**) The size of the ubiquitin-positive inclusions after different dox treatment periods. Purple bars represent results from dox-treated mice, and orange bars represent results obtained from mice with an additional washout after dox induction. $N = 5–7$ mice per group. Significance was determined using a two-tailed *t*-test with 95% confidence interval, with $^{*}P < 0.05$; $^{**}P < 0.01$; $^{***}P < 0.001$; $N = 5–7$ mice per group. Error bars represent SEM.

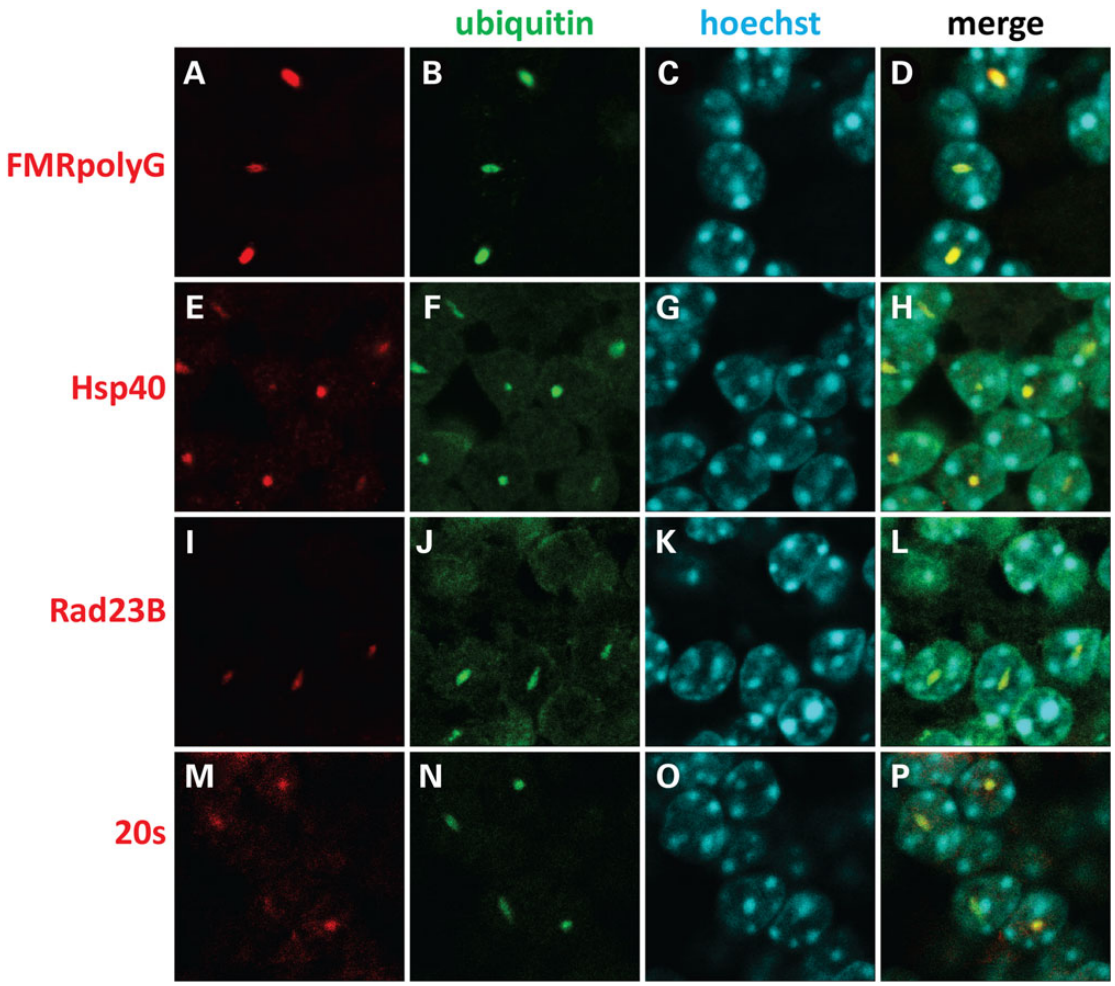

Figure 5. Co-localization of ubiquitin (green) with other components (red) in intranuclear inclusions in the granular cell layer of lobule X of the cerebellum after dox-induced 90CGG RNA expression. Ubiquitin (**B**, **F**, **J** and **N**) co-localizes (**D**, **H**, **L** and **P**) in intranuclear inclusions with FMRpolyG (**A**), Hsp40 (**E**), Rad23B (**I**) and 20S subunit of the proteasome (**M**). Hoechst staining to visualize nuclei (**C**, **G**, **K** and **O**). All images, ×630 magnification.

Reversibility of inclusion formation

The main advantage of the Tet-On system is the ability to shut down transgene expression by removing dox from the drinking water, thus allowing us to study the possibilities of halting and/or reversing disease progression. As we have demonstrated that these inducible mice are a good model to study FXTAS disease progression, we next studied the effect of a wash-out period with normal drinking water after initial dox induction. Importantly, within 48 h of removing dox from the drinking water, we found a rapid decrease in CGG repeat RNA expression, and no significant levels of eGFP could be detected in the brain tissue (Supplementary Material, Fig. S5).

Wash-out periods of 12 weeks were combined with different dox-induction periods of 8, 12 and 16 weeks. For quantification of the number of ubiquitin-positive inclusions before and after washout, we again chose the granular cell layer of cerebellar lobule X. As illustrated in Figure 4, 12 weeks of washout after both 12 and 16 weeks of dox treatment did not result in a significant reduction in the number (Fig. 4A) or size (Fig. 4B) of ubiquitin-positive inclusions in cerebellar lobule X. Nevertheless, we also did not observe an increase in the number or size. Thus, upon stopping expanded CGG repeat RNA expression at these time points appears to prevent further progression of neuropathology. However, 12 weeks of washout after 8 weeks of dox induction resulted in a significant reduction in the number ($P < 0.05$) and size ($P < 0.05$) of inclusions that were still present. Also, after washout, the co-localization of ubiquitin and FMRpolyG in the remaining inclusions remained at 100%, and no single ubiquitin- or FMRpolyG-positive inclusions were observed. Not only the co-localization of FMRpolyG and ubiquitin did not change after washout, but also that of ubiquitin with the 20S proteasome, Hsp40 and Radb23B remained unchanged (data not shown). Thus, we were able to demonstrate reversibility of neuropathology using antibodies against different markers for inclusions.

Development of deficits in compensatory eye movements is halted by dox washout

Based on the high expression of mutant RNA in the granular cell layer of lobule X after dox treatment, one could predict functional deficits and potential functional reversibility in a behavioral test related to this brain region. Lobule X constitutes, together with the two laterally located flocculi, the vestibulo-cerebellum. Although we quantified the inclusions in lobule X, we also found eGFP expression and inclusions in each flocculus. A well-established behavioral test known to be dependent on the flocculus is the optokinetic reflex (OKR). The OKR is a motor reflex driven by full-field visual stimulation that, together with the vestibulo-ocular reflex (VOR), aims to reduce retinal slip (i.e. the movement of visual input across the retina), to ensure clear vision. We tested the effect of the inclusions on this motor behavior in head-fixed mice by presenting a sinusoidally rotating visual stimulus (amplitude 5° and frequency range 0.1–1.0 Hz) while recording their eye movements (Fig. 6B and C). Behavioral effects were analyzed by determining the gain of eye movements, which represents the size of the eye movements relative to the stimulation. Eight weeks of dox induction did not result in a behavioral deficit, as OKR gain was not affected in 90CGG mice [90CGG versus 11CGG, $P = 0.286$, repeated-measures analysis of variance (ANOVA) with Tukey's *post hoc* test] (Fig. 6B). However, prolonged exposure to dox for 20 weeks did result in a behavioral deficit, in that the gain of the OKR in 90CGG mice was lower when compared with that of control mice ($P < 0.001$) and that of mice exposed to dox for only 8 weeks ($P = 0.001$). As the presence of the inclusions is at least partially reversible in lobule X after 8 weeks of dox induction and 12 weeks of washout (Figs 4 and 6A), one could hypothesize that the progression of the behavioral deficits in the OKR could also be attenuated. This was indeed true, because discontinuing the dox induction after 8 weeks of exposure resulted in a better performance at 20 weeks (versus 20 weeks of dox induction, $P < 0.001$), which was no longer

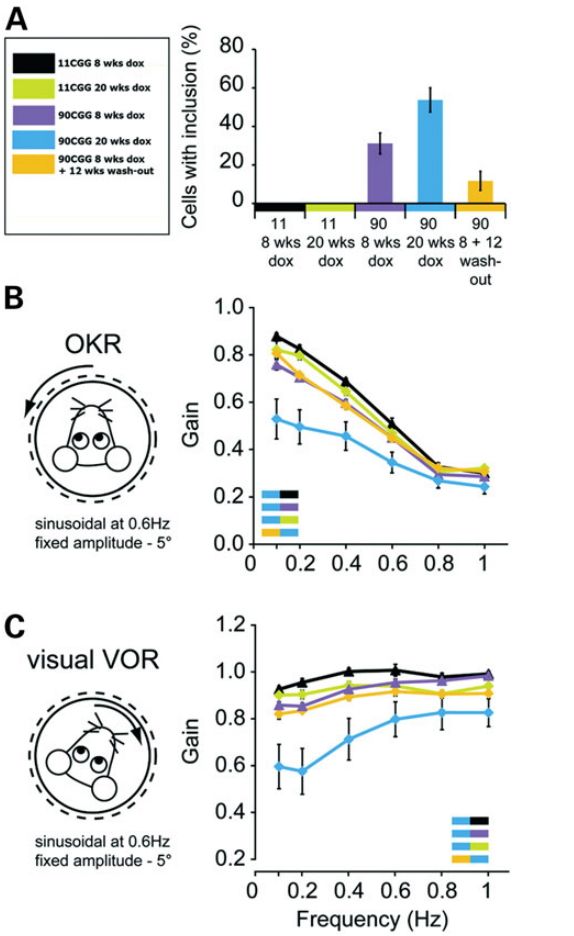

Figure 6. Deficits in the compensatory eye movements correlate with the presence of inclusions. To determine the functional consequences of expanded CGG repeat-induced inclusions, we tested, in head-fixed awake mice, the compensatory eye movements that are known to depend on an intact vestibulo-cerebellum. (**A**) The percentage of nuclei in the granular cell layer of cerebellar lobule X containing an inclusion for mice used in the analysis of compensatory eye movements. (**B**) Sinusoidal rotation of the visual field evoked the OKR, a cerebellum-dependent reflex that minimizes retinal slip. The OKR gain, the ratio of eye-to-stimulus velocity, over a range of frequencies, was compared between mice with and without (ir)reversible inclusions. Whereas gains of 90CCG mice after 8 weeks of dox induction (purple) were not significantly lower than those in controls (black), irreversible inclusions as a result of 20 weeks of exposure to dox (blue) did cause deficits in eye movement performance compared with controls (yellow). In contrast, reversing the presence of inclusions by washout (8 weeks of dox induction followed by 12 weeks of washout, orange) prevented the development of performance deficits. (**C**) In everyday life, the OKR works in conjunction with the VOR, to maintain a stable image on the retina. To test whether the deficits in the OKR could also affect more natural behaviors, mice were subjected to sinusoidal rotation of the turntable in the light, to evoke the VVOR. All the differences present in the OKR were reproduced, confirming the link of inclusions with behavioral deficits. Insets, colors indicate comparisons with $P < 0.05$ (repeated-measures ANOVA followed by Tukey's *post hoc*).

significantly different from that of control mice (versus 11CGG with 20 weeks of dox induction, $P = 0.993$). When we tested OKR gains evoked by visual stimulation with fixed velocity (8°/s and frequencies 0.05–1.6 Hz), instead of fixed amplitude, the same differences were found (Supplementary Material, Fig. S6), strengthening our conclusion that dox exposure correlates with cerebellum-dependent functional deficits.

As described earlier, the OKR is used in conjunction with the VOR, a reflex based on vestibular input from the semi-circular canals to generate the visually enhanced reflex or VVOR. The VVOR functions to stabilize an image on the retina when moving through an environment. To verify whether the deficits in OKR are compensated by changes in the processing of vestibular input, we also tested the VOR and VVOR in the same mice (Fig. 6B and Supplementary Material, Fig. S6B). The VOR, evoked by head rotation in the dark, can be influenced by, but does not require, the cerebellum. In line with that, the differences in VOR gain were, compared with those in OKR gain, in the same general direction, but less pronounced (Supplementary Material, Fig. S6B). In VVOR gain, similar to OKR, we observed a significantly lower gain in mice with irreversible inclusions after prolonged, 20-week dox exposure (90CGG versus 11CGG, $P = 0.002$ and 20 versus 8 weeks of dox in 90CGG, $P = 0.020$). Here too, this deficit could be prevented by stopping the dox exposure after 8 weeks (20 weeks dox versus washout in 90CGG, $P = 0.004$).

To conclude, the presence of irreversible inclusions in the vestibulo-cerebellum correlates with deficits in compensatory eye movements, which depends on their proper functioning. Reversing inclusion number and size by ceasing dox induction after 8 weeks of exposure minimized disease progress, in that the compensatory eye movements did not deteriorate further.

Discussion

Several animal models have contributed to understanding of the molecular mechanisms underlying FXTAS and have characterized the disease process. However, previous mouse models did not make it possible to address questions concerning the possible reversibility of FXTAS or to elucidate critical periods in the natural history of the disease (13). In order to address such questions, we describe the successful development and initial characterization of an inducible mouse model for the fragile X-premutation and FXTAS. In this model, an expanded CGG RNA is expressed under control of a Tet-On promoter activated by the addition of dox to drinking water (14). This inducible model shows no evidence of expression in the absence of dox (i.e. no leakage of expression) and allows us to control the timing of CGG RNA expression during development. Consequently, we were able not only to examine disease progression in these mice, but also to provide evidence for the potential for halting disease progression and reversal of neuropathology and specific functional deficits. Specifically, the number and size of inclusions formed in these mice by induced expression of expanded CGG RNA were reversible when mice were exposed to dox starting from 3 weeks of age and taken off dox after 8 weeks of exposure. However, reversibility could only be demonstrated after 8 weeks of dox treatment and not after longer treatment periods of 12 and 16 weeks. This study shows that the *in vivo* formation of inclusions is dependent on the expression of an RNA bearing an expanded CGG repeat rather than on overexpression of CGG RNA *per se*. Finally, the aberrant behavior of these mice in an eye reflex test did not deteriorate further when expression of the expanded CGG RNA was stopped by withdrawal of dox exposure. Our results, therefore, suggest that only an early intervention may be beneficial for FXTAS patients and premutation carriers.

The major histopathological hallmark of FXTAS is the presence of ubiquitin-positive intranuclear inclusions in neurons and astrocytes seen in the post-mortem brain. We therefore focussed on their presence in the quantitative analysis of this new inducible mouse model. In the cerebellum, where we focussed our quantitative analyses, we found clear evidence that the number and size of the inclusions increased with longer exposure to dox. It remains to be seen whether these inclusions are pathological or protective in the brain. However, we recently reported that dox-induced expression of expanded CGG RNA can cause mitochondrial damage in the liver, followed by early death of mice within 1 week of exposure. These experiments were carried out in bigenic mice (TRE-90CGG-eGFP/hnRNP-rtTA), in which expression of the expanded CGG RNA utilized an hnRNP promoter to drive rtTA expression (14). Importantly, these bigenic mice express elevated levels of mutant-expanded CGG RNA in the liver, but show a total absence of ubiquitin-positive inclusions. On the basis of these results, free expanded CGG RNA appears to be toxic, even in the absence of inclusions. This finding does not, however, exclude the possibility that, in human brain, the formation of intranuclear inclusions and subsequent sequestration of specific RNA-binding proteins can also interfere with normal cell functioning, which could then ultimately lead to cell death (4).

The main hypothesis for the cause of FXTAS has been an RNA toxic gain-of-function mechanism, in which high levels of expression of RNA bearing an expanded CGG repeat are the primary mechanism of pathology. This hypothesis is consistent with the fact that the expanded CGG repeat is present in the 5′-UTR of the *FMR1* gene and is therefore not translated into protein. However, for different repeat-associated disorders, including FXTAS, frontotemporal dementia (FTD) and amyotrophic lateral sclerosis (ALS), a new alternative translational mechanism has been described (reviewed in 16), reopening the discussion about the mechanism of pathology. Specifically, repeat-associated non-AUG (RAN) translation of the trinucleotide repeat has been reported, resulting in the presence of FMRpolyG and FMRpolyA (8).

In this study, we have shown the presence of the RAN translation product FMRpolyG in the ubiquitin-positive inclusions. The observation that inclusions are pathogenic and contain the FMRpolyG peptide is consistent with a role for the polypeptide in disease pathology. Of course, this finding does not rule out a role for *Fmr1* RNA toxicity in the inclusion formation. Although the gain-of-function mechanism of pathology therefore remains possible in FXTAS, it might involve both RNA and protein. For the expanded hexanucleotide repeat (GGGGCC) involved in ALS and FTD, it has now been shown in *Drosophila* that toxicity seems to be caused by certain dipeptide repeats rather than by the repeat RNA (17). Such models are not yet available for FXTAS, but research is ongoing to establish the roles of different entities in FXTAS pathology.

The presence of Hsp40, Rad23B and the 20S subunit of the proteasome in the inclusions again suggests a role for the proteasomal degradation pathway in inclusion formation, as was found for other FXTAS mouse models (12,15,18). The involvement of the proteasome is 2-fold. First, the proteasome is overloaded with the ubiquitinated proteins present in the inclusions that it should degrade. Secondly, components of the proteasome itself are sequestered in the inclusions and therefore cannot optimally perform its function. The involvement of the proteasome in pathology is not unique for FXTAS, but is a general process involved in several neurodegenerative diseases with which FXTAS may share common disease mechanisms.

To evaluate the functional consequences of the inclusions in the cerebellum of the dox-treated bigenic inducible mice, we quantified reflexive eye movements associated with cerebellar lobule X, which showed high levels of expanded CGG RNA expression. The compensatory eye movements evoked by full-field visual stimulation or head rotation are known as the OKR and VVOR, respectively. These eye movements are controlled by the vestibulo-cerebellum, the region of the brain in which most inclusions were observed. The prominent presence of irreversible inclusions after 20 weeks of dox exposure could be linked to motor performance deficits, in that the gain of the OKR and VVOR was lower in these mice. In fact, the compensatory eye movements in mice treated for 8 weeks with dox already appear to be affected. Although this difference was not statistically significant in the overall group comparison, the differences were statistically significant when individual groups were compared for each reflex (OKR: $P = 0.0013$ and VVOR: $P = 0.0002$). This suggests that the phenotype worsens over time in these inducible mice, with an accompanying increase in the number and size of inclusions, whereas transgene RNA expression levels remain the same. These ocular reflexes nicely model the progressive character of FXTAS disease development and suggest that the inclusions coincide with disease symptoms in specific brain regions. Ending the exposure to dox after 8 weeks effectively reversed the disease progress in terms of inclusions and prevented the progressive deterioration of the OKR and VVOR gains. The finding that the development of more severe motor performance deficits could be prevented by halting the expression of the expanded repeat emphasizes the potential benefit of early intervention.

Regardless of whether FXTAS is caused by RNA directly or by translation of a toxic protein, the results of this study demonstrate that it is possible to halt or even reverse disease progression if expression of the RNA carrying the expanded CGG repeat is stopped. Translating the time course of disease from a transgenic mouse to the human situation is difficult, but what is clear from the present research is that therapeutic intervention in FXTAS patients and premutation carriers is possible. After longer intervals, we observed that stopping expanded CGG RNA expression stops further disease progression; earlier in the process even reversibility of pathology is possible.

The early time point at which we found reversibility suggests that it might be needed to treat asymptomatic premutation carriers, which raises the ethical question of whom to treat and when to start. Therefore, research will also need to focus on identifying biomarkers to predict which premutation carriers are most likely to develop FXTAS. However, later intervention might also be promising to prevent further disease progression. Therefore, for all FXTAS patients, it is important to investigate whether interfering with the expanded CGG RNA expression is possible. Although it may be a long time before effective therapeutic interventions for FXTAS are available for clinical use, the results of these experiments—reversibility of disease pathogenesis—represent a 'proof of principle' that effective treatments are possible. This is a very important step in recognizing the options and opens new avenues for further research for other repeat-related diseases involving gain-of-function mechanisms caused by RAN translation or RNA.

Materials and Methods

Mouse lines, dox treatment and genotyping

TRE-11CGG-eGFP and TRE-90CGG-eGFP mouse strains and genotyping were as described previously (14) in C57BL/6JRj (from Janvier Labs) background. The TRE-90CGG-eGFP mouse strain has been bred for several generations, and never any instability of the repeat size was observed. In this study, PrP-rtTA was used as the driver to induce expression. The PrP-rtTA transgene was cloned by inserting rtTA2S-MS (a kind gift from H. Bujard) into the MoPrP.Xho vector using the *Xho*I restriction sites. Transgenic mice were generated by injecting linearized constructs into oocytes of C57BL/6JRj (from Janvier Labs) mice. We had six founders and used the one with the highest expression level and broadest expression pattern. PrP-rtTA mice were cross bred with TRE-nCGG-eGFP mice to obtain bigenic mice. Genotyping of the mice was performed, as described previously (14). Dox treatment of bigenic mice started directly after weaning at an age of 3–4 weeks. Dox (Sigma, Zwijndrecht, the Netherlands) was added to the drinking water in a concentration of 4 mg/ml, supplemented with 5% sucrose. Drinking water was kept from the light and refreshed every 2–3 days. Mice were treated with dox for 8, 12, 16, 22 or 28 weeks. If a wash-out period was added after dox induction, mice received standard drinking water during the 12 weeks after their dox treatment. All experiments were conducted with the permission of the local animal welfare committee (DEC).

RNA isolation and quantitative RT-PCR

RNA isolation was performed as described previously (14). Briefly, brains were homogenized in 4-(2-hydroxyethyl)-1-piperazineethanesulfonic acid buffer pH 7.6 containing 0.45% Triton X-100, 0.05% Tween-20 and protease inhibitors. RNA was isolated using RNA Bee, according to manufacturer's instructions. Quantitative RT-PCR was performed on cDNA synthesized with iScript (Biorad, Veenendaal, the Netherlands), according to the manufacturer's instructions, using KAPA SYBR Green (KAPA Biosystems, London, UK) on a Biorad CFX machine.

Immunohistochemistry and immunofluorescence

Tissues were fixed overnight in 4% paraformaldehyde and embedded in paraffin according to standard protocols. Sections (6 µm) were deparaffinized followed by antigen retrieval using microwave treatment in 0.01 M sodium citrate. Endogenous peroxidase activity was blocked, and immunostaining was performed overnight at 4°C using mouse anti-GFP (Roche 1814460; 1:1000), rabbit anti-ubiquitin (Dako Z0458; 1:250) or mouse anti-FMRpolyG (8FM (9); 1:10) antibodies. Antigen–antibody complexes were visualized by incubation with DAB substrate (Dako), after incubation with Brightvision poly-HRP-linker (Immunologic). Slides were counterstained with hematoxylin and mounted with Entellan.

Inclusions were quantified by counting 500 nuclei of the granular cell layer of lobule X of the cerebellum and by counting the number of ubiquitin-positive inclusions at a 100× magnification. The size of the inclusions was determined using an Olympus BX40 microscope at a 100× magnification and cellSens Dimension software. Researchers were blinded for genotype and treatment. If lobule X was not present in paraffin sections, mice were excluded resulting in the use of five to seven mice for each group. This number was used based on the previous research (12,19); both male and female littermates were randomly distributed over the different groups.

For (double) immunofluorescence, slides were blocked for autofluorescence with Sudan Black in 70% ethanol. Primary antibodies include rabbit anti-ubiquitin (DAKO Z0458; 1:50), mouse anti-ubiquitin (Cytoskeleton AUB01-S; 1:200), mouse anti-FMRpolyG (1:10) (9), rabbit anti-Hsp40 (Stressgen SPA-400;

1:100), rabbit anti-Rad23B (1:100) (15) or rabbit anti-20S subunit of the proteasome (1:100) (12). Secondary antibodies include anti-rabbit Fab Alexa 488 (Life technologies A11070; 1:100) and anti-mouse Cy3 (Jackson ImmunoResearch 715-165-150; 1:100). Nuclei were visualized with Hoechst. Analysis was performed with a Leica confocal microscope and LAS AF software.

Compensatory eye movements

Male mice, aged 7 or 19 weeks, were surgically prepared for chronic, head-restrained recordings of compensatory eye movements, as described previously (20,21). Based on this previous research, 9–13 mice per group were used, and littermates were randomly divided over the different groups. In short, under isoflurane anesthesia (initiation at 4% and maintenance at ~1.5%, with O_2), a construct was attached to the skull in parallel to the intracranial midline using Optibond primer and adhesive (Kerr) and Charisma (Haeraeus Kulzer). The construct consisted of a brass holder with magnet (neodymium, 4 × 4 × 2 mm, MTG Europe) inside. After a recovery period (≤3 days), mice were head-fixed to a metal bar using the magnet embedded in the pedestal, a complementary magnet in the bar and a securing screw. The body of the mouse was placed in a custom-made cylindrical restrainer and the head centered in the middle of a turntable. A cylindrical screen (diameter 63 cm) with a random-dotted pattern (each element 2°) surrounded the turntable (diameter 60 cm), on which the mouse was placed. The OKR and VOR in the dark and in the light (VVOR) were elicited by sinusoidal rotation of either the drum (OKR) or the table (VOR and VVOR), respectively. Eye movement performance was tested by rotating the drum or table at 0.1–1.0 Hz with 5° amplitude (fixed) or the drum at 0.05–1.6 Hz at 8°/s peak velocity (fixed). Each frequency–amplitude combination was tested twice with 8–20 repeated cycles, and results were averaged. To illuminate the eye during the recordings, we used two table-fixed infrared emitters (maximum output 600 mW, dispersion angle 7° and peak wavelength 880 nm) and a third emitter mounted on the camera aligned horizontally with the camera's optical axis. The third emitter produced the tracked corneal reflection. The pupil position, after subtraction of the corneal reflecting position, was recorded using eye-tracking software (ETL-200, ISCAN Systems, Burlington, NA, USA). Calibrations were performed, as described previously (22). Gain and phase values of the eye movements were calculated using a custom-made Matlab routine (Matlab, MathWorks Inc.).

Statistics

Statistical significance of the QRT-PCR results was analyzed using a Student's *t*-test. The quantification and size determination of the inclusions and results were statistically analyzed with a univariate ANOVA and a subsequent Tukey's *post hoc* test. For the analysis of the compensatory eye movements, gain and phase results plotted against frequency or time were statistically analyzed using repeated-measures ANOVA followed by Tukey's *post hoc* test.

Supplementary Material

Supplementary Material is available at *HMG* online.

Acknowledgement

The authors wish to thank Hermann Bujard for the gift of the rtTA2S-MS construct and Tom de Vries Lentsch, Christina Merakou, Fatwa Adikusuma and Laura Ashley van Dijk for their contributions.

Conflict of Interest statement. The authors declare that they have no conflicts of interest.

Funding

This work was supported by E-Rare (ZonWM project 113301201 to R.K.H. and ZonWM project 113301401 to R.W.); the Netherlands Brain Foundation [F2012(1)-101 to R.W. and F2015(1)-02 to R.K.H.]; National Institutes of Health (NINDS RO1 NS079775 to R.F.B. and R.W., NIA RL1 NS062411 to R.F.B., NIDCR UL1 DE019583 to R.F.B. and P.J.H. and NIA RL1 AG032119 to P.J.H.); NOW—Life Sciences VENI (to M.S.); ERC-Advanced to (C.I.D.Z.); Neurobasic (to C.I.D.Z.); ZonWM (to C.I.D.Z.) and NWO-ALW (to C.I.D.Z.).

References

1. Hagerman, R.J., Leehey, M., Heinrichs, W., Tassone, F., Wilson, R., Hills, J., Grigsby, J., Gage, B. and Hagerman, P.J. (2001) Intention tremor, parkinsonism, and generalized brain atrophy in male carriers of fragile X. *Neurology*, **57**, 127–130.
2. Hunter, J., Rivero-Arias, O., Angelov, A., Kim, E., Fotheringham, I. and Leal, J. (2014) Epidemiology of fragile X syndrome: a systematic review and meta-analysis. *Am. J. Med. Genet. A.*, **164A**, 1648–1658.
3. Rodriguez-Revenga, L., Madrigal, I., Pagonabarraga, J., Xuncla, M., Badenas, C., Kulisevsky, J., Gomez, B. and Mila, M. (2009) Penetrance of FMR1 premutation associated pathologies in fragile X syndrome families. *Eur. J. Hum. Genet.*, **17**, 1359–1362.
4. Greco, C.M., Berman, R.F., Martin, R.M., Tassone, F., Schwartz, P.H., Chang, A., Trapp, B.D., Iwahashi, C., Brunberg, J., Grigsby, J. *et al.* (2006) Neuropathology of fragile X-associated tremor/ataxia syndrome (FXTAS). *Brain*, **129**, 243–255.
5. Tassone, F., Hagerman, R.J., Taylor, A.K., Gane, L.W., Godfrey, T.E. and Hagerman, P.J. (2000) Elevated levels of FMR1 mRNA in carrier males: a new mechanism of involvement in the fragile-X syndrome. *Am. J. Hum. Genet.*, **66**, 6–15.
6. Hagerman, P. (2013) Fragile X-associated tremor/ataxia syndrome (FXTAS): pathology and mechanisms. *Acta Neuropathol.*, **126**, 1–19.
7. Zu, T., Gibbens, B., Doty, N.S., Gomes-Pereira, M., Huguet, A., Stone, M.D., Margolis, J., Peterson, M., Markowski, T.W., Ingram, M.A. *et al.* (2011) Non-ATG-initiated translation directed by microsatellite expansions. *Proc. Natl Acad. Sci. USA*, **108**, 260–265.
8. Todd, P.K., Oh, S.Y., Krans, A., He, F., Sellier, C., Frazer, M., Renoux, A.J., Chen, K.C., Scaglione, K.M., Basrur, V. *et al.* (2013) CGG repeat-associated translation mediates neurodegeneration in fragile X tremor ataxia syndrome. *Neuron*, **78**, 440–455.
9. Buijsen, R.A., Sellier, C., Severijnen, L.A., Oulad-Abdelghani, M., Verhagen, R.F., Berman, R.F., Charlet-Berguerand, N., Willemsen, R. and Hukema, R.K. (2014) FMRpolyG-positive inclusions in CNS and non-CNS organs of a fragile X premutation carrier with fragile X-associated tremor/ataxia syndrome. *Acta Neuropathol. Commun.*, **2**, 162.
10. Bontekoe, C.J., Bakker, C.E., Nieuwenhuizen, I.M., van Der Linde, H., Lans, H., de Lange, D., Hirst, M.C. and Oostra, B.A. (2001) Instability of a (CGG)(98) repeat in the Fmr1 promoter. *Hum. Mol. Genet.*, **10**, 1693–1699.
11. Entezam, A., Biacsi, R., Orrison, B., Saha, T., Hoffman, G.E., Grabczyk, E., Nussbaum, R.L. and Usdin, K. (2007) Regional

FMRP deficits and large repeat expansions into the full mutation range in a new fragile X premutation mouse model. *Gene*, **395**, 125–134.
12. Willemsen, R., Hoogeveen-Westerveld, M., Reis, S., Holstege, J., Severijnen, L., Nieuwenhuizen, I., Schrier, M., VanUnen, L., Tassone, F., Hoogeveen, A. *et al.* (2003) The FMR1 CGG repeat mouse displays ubiquitin-positive intranuclear neuronal inclusions: implications for the cerebellar tremor/ataxia syndrome. *Hum. Mol. Genet.*, **12**, 949–959.
13. Berman, R.F., Buijsen, R.A., Usdin, K., Pintado, E., Kooy, F., Pretto, D., Pessah, I.N., Nelson, D.L., Zalewski, Z., Charlet-Bergeurand, N. *et al.* (2014) Mouse models of the fragile X premutation and fragile X-associated tremor/ataxia syndrome. *J. Neurodev. Disord.*, **6**, 25.
14. Hukema, R.K., Buijsen, R.A., Raske, C., Severijnen, L.A., Nieuwenhuizen-Bakker, I., Minneboo, M., Maas, A., de Crom, R., Kros, J.M., Hagerman, P.J. *et al.* (2014) Induced expression of expanded CGG RNA causes mitochondrial dysfunction *in vivo*. *Cell Cycle*, **13**, 2600–2608.
15. Bergink, S., Severijnen, L.A., Wijgers, N., Sugasawa, K., Yousaf, H., Kros, J.M., van Swieten, J., Oostra, B.A., Hoeijmakers, J.H., Vermeulen, W. *et al.* (2006) The DNA repair-ubiquitin-associated HR23 proteins are constituents of neuronal inclusions in specific neurodegenerative disorders without hampering DNA repair. *Neurobiol. Dis.*, **23**, 708–716.
16. Wojciechowska, M., Olejniczak, M., Galka-Marciniak, P., Jazurek, M. and Krzyzosiak, W.J. (2014) RAN translation and frameshifting as translational challenges at simple repeats of human neurodegenerative disorders. *Nucleic Acids Res.*, **42**, 11849–11864.
17. Mizielinska, S., Gronke, S., Niccoli, T., Ridler, C.E., Clayton, E.L., Devoy, A., Moens, T., Norona, F.E., Woollacott, I.O., Pietrzyk, J. *et al.* (2014) C9orf72 repeat expansions cause neurodegeneration in *Drosophila* through arginine-rich proteins. *Science*, **345**, 1192–1194.
18. Hashem, V., Galloway, J.N., Mori, M., Willemsen, R., Oostra, B.A., Paylor, R. and Nelson, D.L. (2009) Ectopic expression of CGG containing mRNA is neurotoxic in mammals. *Hum. Mol. Genet.*, **18**, 2443–2451.
19. Brouwer, J.R., Huizer, K., Severijnen, L.A., Hukema, R.K., Berman, R.F., Oostra, B.A. and Willemsen, R. (2008) CGG-repeat length and neuropathological and molecular correlates in a mouse model for fragile X-associated tremor/ataxia syndrome. *J. Neurochem.*, **107**, 1671–1682.
20. Schonewille, M., Gao, Z., Boele, H.J., Veloz, M.F., Amerika, W.E., Simek, A.A., De Jeu, M.T., Steinberg, J.P., Takamiya, K., Hoebeek, F.E. *et al.* (2011) Reevaluating the role of LTD in cerebellar motor learning. *Neuron*, **70**, 43–50.
21. Galliano, E., Gao, Z., Schonewille, M., Todorov, B., Simons, E., Pop, A.S., D'Angelo, E., van den Maagdenberg, A.M., Hoebeek, F.E. and De Zeeuw, C.I. (2013) Silencing the majority of cerebellar granule cells uncovers their essential role in motor learning and consolidation. *Cell Rep.*, **3**, 1239–1251.
22. Stahl, J.S., van Alphen, A.M. and De Zeeuw, C.I. (2000) A comparison of video and magnetic search coil recordings of mouse eye movements. *J. Neurosci. Methods*, **99**, 101–110.